Impact of Dimethyl Sulfoxide Treatment on Morphology and Characteristics of Nanofibrillated Cellulose Isolated from Corn Husks

Xue Yang,[a] Xiaoting Wang,[a] Hui Liu,[a] Yanjiao Zhao,[a] Shuai Jiang,[a] and Lifang Liu [a,b,*]

This work investigated the impact of dimethyl sulfoxide (DMSO) treatment in the isolation of nanofibrillated cellulose (NFC) from corn husk by the 2,2,6,6,-tetramethylpilperidine-1-oxyl (TEMPO) oxidation method. NFC-A and NFC-B were prepared without and with DMSO treatment before TEMPO oxidation. The extracted NFC were characterized by scanning electron microscopy (SEM), transmission electron microscopy (TEM), Fourier transform infrared spectroscopy (FTIR), zeta potential analyzer, X-ray diffraction (XRD), and thermogravimetric analysis (TGA). The results showed that the dimension of both NFC-A and NFC-B were in nanoscale. The crystalline type of NFC was cellulose I, and the crystallinity of NFC was obviously increased. The thermal stability of NFC was reduced slightly. Compared with NFC-A, NFC-B had a narrower distribution range, higher crystallinity, and better thermal stability. This result demonstrated that DMSO treatment did not change the chemical structure of NFC, but it affected their dimension and distribution and improved their dispersion stability, crystallinity, and thermal stability.

Keywords: Corn husk; Nanofibrillated Cellulose; TEMPO-oxidation; Dimethyl sulfoxide (DMSO)

Contact information: a: College of Textiles, Donghua University, Shanghai, 201620 China; b: The Key Lab of Textile Science & Technology, Ministry of Education, Donghua University, Shanghai 201620 China;
** Corresponding author: lifangliu@dhu.edu.cn*

INTRODUCTION

Nanofibrillated cellulose (NFC) is a nanomaterial isolated from cellulose resources. NFC particles are characterized by diameters between 5 nm to 60 nm and lengths on the micrometer scale, and they are comprised of both amorphous and crystalline regions of cellulose (Carpenter *et al.* 2015). In addition to many sources of cellulose, biodegradability, and renewability, NFC particles have many considerable features and characteristics, such as abundant surface hydroxyl groups, large specific surface area, high aspect ratio, high crystallinity, low density, good mechanical properties, high thermal stability, and good optical properties (Ng *et al.* 2015). Due to their unique properties and nanoscale effects, NFC may be used in many applications such as nanocomposites, paper making, coating additives, security papers, food packaging, gas barriers, and pharmacy.

NFC has been isolated from various lignocellulosic sources, such as wood (Salmela *et al.* 2008), cotton fiber (Do Nascimento *et al.* 2015), sisal fiber (Moran *et al.* 2008), bamboo residue (Wang *et al.* 2015), tunicate cellulose (Zhang *et al.* 2013), and bacterial cellulose (Grunert and Winter 2002). Recently, agricultural wastes, such as rice straw, rapeseed straw, and corn stalks (Chaker *et al.* 2014) have received increasing attention as potentially renewable sources for NFC production. They have shorter growing cycles and lower lignin contents compared with woody fiber sources, and they can be disintegrated

into NFC with less severe delignification processes. NFC isolation from different agricultural wastes is of both industrial and scientific importance due to the large variety of lignocellulosic raw materials around the world.

Corn is one of the most widely distributed crops in the world. However, corn husks, the outer covering of the corn, are not used efficiently. Corn husks are commonly burned or buried; this wastes resources and causes environmental pollution. Therefore, utilization of this low-value material for a high-value application will have an important effect on energy saving, environment protection, and economic development. Corn husks are made of lignocellulosic materials. Cellulose and hemicellulose are the major components of corn husks comprising 827 g/kg of its dry matter (Barl *et al.* 1991). The extraction of NFC from corn husks improves their economic value. Different methods have been used to extract NFC from corn husk (Mendes *et al*. 2015; Du *et al.* 2016; Xiao *et al.* 2016).

The 2,2,6,6,-tetramethylpilperidine-1-oxyl (TEMPO) oxidation method selectively introduces carboxyl groups at the C_6 of glucose, efficiently generating NFC with a uniform size; TEMPO does not change the crystallographic forms of the starting cellulosic materials, which is beneficial to NFC application (Saito *et al.* 2007; Isogai *et al.* 2011; Miao *et al.* 2016). Therefore, TEMPO oxidation method is one of the most widely used approaches for NFC extraction. Dimethyl sulfoxide (DMSO) treatment is a pretreatment process before TEMPO oxidation in some research (Cao *et al.* 2012; Miao *et al*. 2016), while DMSO pretreatment has been omitted in other research (Yu *et al.* 2014; Du *et al.* 2016). The effect of DMSO treatment on the morphology and properties of NFC has not been fully investigated. And the mechanism of DMSO for the preparation of NFC has never been researched before.

The focus of this work was to study the mechanism of DMSO for the preparation of NFC and the impact of DMSO treatment on the morphology and properties of NFC. Corn husks were used as raw materials to prepare NFC by the TEMPO method. The purified cellulose powders (CPs) were treated with or without DMSO before the TEMPO oxidation process. In order to explore the mechanism of DMSO for the preparation of NFC, ethanol and acetone were also used to deal with CPs according to DMSO treatment conditions. The prepared CPs and NFC were investigated by scanning electron microscopy (SEM), transmission microscopy (TEM), zeta potential analyzer, Fourier transform infrared spectroscopy (FTIR), X-ray diffraction (XRD), and thermogravimetric analysis (TGA).

EXPERIMENTAL

Raw Materials

Corn husks were collected from a farm in Binzhou, China. The corn husks were washed with tap water to remove sand and other impurities and then air-dried under ambient conditions.

Chemical Reagent

TEMPO and DMSO were purchased from Aladdin Chemistry Co. Ltd., Shanghai, China. The other chemicals were purchased from Sinopharm Chemical Reagent Co., Ltd., Shanghai, China. All chemicals were of analytical or reagent grades.

Methods

Preparation of cellulose fibers from corn husks

The washed and air-dried corn husks were cut into small pieces and soaked in 10 g/L penetrant solution for 72 h. The residual penetrant was removed completely by repeated washing with deionized water. The corn husks were added to a 3 g/L solution of sulfuric acid for 2 h with an acid to corn husk weight ratio of 50 mL/g, and the residual acid solution was removed with deionized water. The corn husks were boiled according to the sourcing process condition I in Table 1, followed by repeated washing with deionized water. Finally, the cellulose fibers were prepared in accordance with Scouring II, as shown in Table 1, to further remove the non-cellulose materials. The residual chemicals were rinsed with deionized water.

Table 1. Scouring Process Conditions

Reagent and Process Conditions	Scouring I	Scouring II
Sodium hydroxide (wt.%)	0.3	0.6
Sodium silicate (wt.%)	0.24	0.08
Sodium carbonate anhydrous (wt.%)	0.56	0.48
Sodium sulfite anhydrous (wt.%)	0.3	0.36
Sodium pyrophosphate (wt.%)	0.08	0.32
Sodium polyphosphate (wt.%)	0.08	0.16
Penetrant (g/L)	5	5
Temperature (°C)	100	100
Time (min)	60	60

Preparation of NFC from cellulose fibers

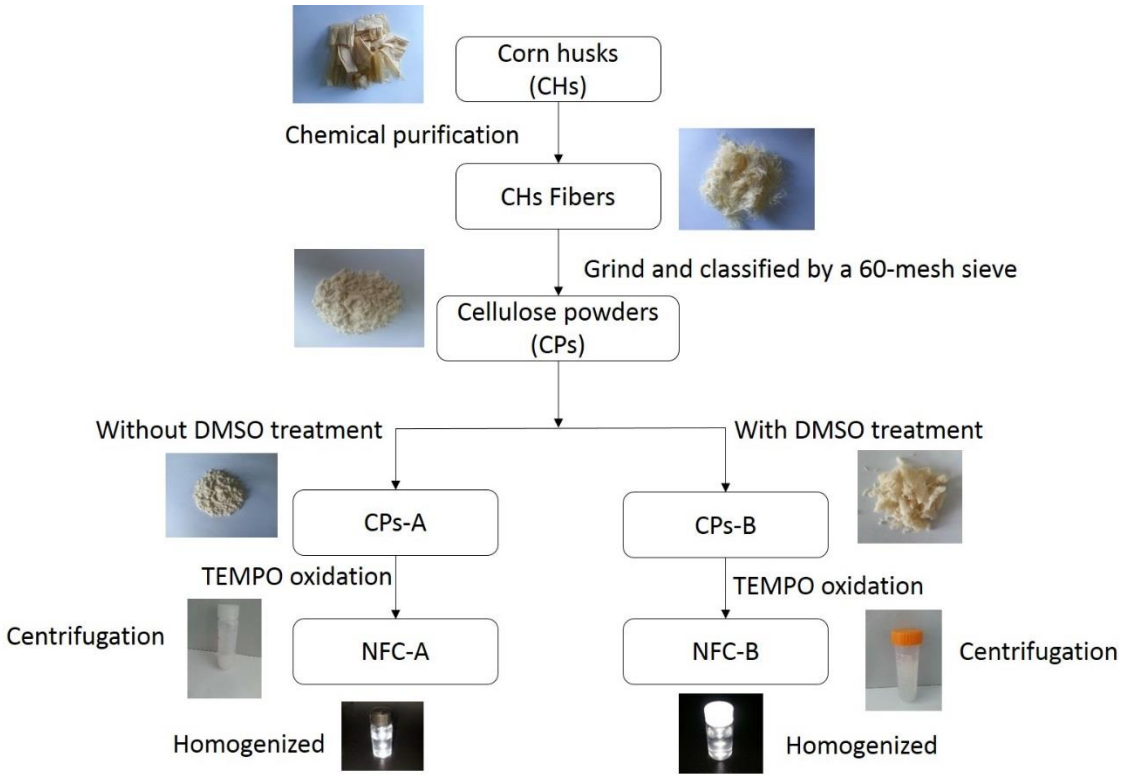

Fig. 1. Schematic representation of the NFC extracted from corn husks

Figure 1 describes the preparation process of NFC extracted from cellulose fibers. The cellulose fibers were ground into a powder using a DJ-04 grinder (Shanghai Dianjiu Traditional Medicine Machinery Manufacture Co., Ltd, Shanghai, China) and classified using a 60-mesh sieve. The cellulose powder (CPs) without DMSO treatment was named CPs-A. CPs was mixed with DMSO (powders to liquid ratio of 1:30) for chemical swelling using a magnetic hot plate stirrer at 60 °C for 5 h under 600 rpm stirring. The suspension was washed with deionized water repeatedly using a SHZ-D (III) suction filter machine (Tianjin Huaxin Instrument factory, Tianjin, China), until the DMSO solution was washed out completely. After filtration, the wet CPs was dried in a vacuum drying oven at 50 °C for 6 h. The CPs after DMSO treatment was denoted as CPs-B.

NFC particles were prepared from CPs-A and CPs-B, which were named as NFC-A and NFC-B, respectively. The procedure were as follows: 1 g of dried CPs-A was mixed with 100 mL deionized water and stored at 4 °C for 3 h. Next, 0.032 g of TEMPO and 0.636 g of NaBr were added to the mixture. The solution was mixed uniformly with a magnetic stirrer at 600 rpm, while 40 mL NaClO was added dropwise; 5 wt.% HCl was added to adjust the mixture to pH 10.5. The mixture was stirred at 600 rpm for 2 h. The reaction was stopped by adding 5 mL anhydrous ethanol. The TEMPO-oxidized suspension was centrifuged in a H1650 supercentrifuge (Hunan Xiangyi Laboratory Instrument development Co., Ltd, Changsha, China) at 5000 rpm for 15 min to recover the precipitate. The precipitate was suspended in deionized water, followed by centrifugation. This process was repeated until the supernatant solution became turbid. The colloidal suspension was collected and homogenized for 5 min using an IKA T25 digital Ultra-Turrax (IKA Laboratory technology Co., Ltd, Staufen, Germany). The resulting suspension was stored in a refrigerator at 4 °C and denoted as NFC-A; 1 g of dried CPs-B was used, repeating the other procedure mentioned above, thus giving rise to NFC-B.

Characterization

The chemical composition of corn husks (CHs) and cellulose powders (CPs) was tested according to the GB 5889 (1986) standard. The zeta potential was measured with a Nano-ZS particle size & zeta potential analyzer (Malvern Instrument Co., Ltd, Shanghai, China).The Fourier transform infrared (FTIR) spectrograms were recorded with a Nicolet 8700 FTIR spectrometer (Thermo Fisher Scientific Co., Ltd, Waltham, MA, USA) in the range of 650 to 4000 cm^{-1} with a step of 0.5 cm^{-1}. The morphology was analyzed using JSM-5600LV SEM (JEOL Ltd, Tokyo, Japan) and JEM-2100 TEM (JEOL Ltd, Tokyo, Japan) devices. The crystallinity of the cellulose samples was examined with an D/MAX 2550PC XRD (Rigaku, Tokyo, Japan) with a monochromatic Cu Kα radiation source in the step-scan mode, with a 2θ angle ranging from 5 ° through 60 ° and a step of 0.02 °. The thermal property was analyzed with TG209F1 analyzer (NETZSCH Instrument Trading Ltd, Selb, Germany) under a N_2 atmosphere with gas flow rate of 20 mL/min, heating temperature range from 50 °C to 600 °C, and a heating rate of 10 °C/min.

RESULTS AND DISCUSSION

Chemical Analysis

The chemical composition of corn husks (CHs) and cellulose powders (CPs) is listed in Table 2. Cellulose content in CHs was 20%, while the amount of hemicellulose and lignin were 46.46% and 19.06%, respectively. CHs also contained a small amount of

wax, hydrotrope, and pectin. After the chemical purification treatment, the composition of CPs-A had noticeable changes. The cellulose content in CPs-A increased from 20.00% to 49.74%, while hemicellulose decreased from 46.46% to 24.25%. Lignin decreased from 19.06% to 16.24%. The wax, pectin, and hydrotrope contents were also reduced. This shows most of the non-cellulose materials were removed during the chemical purification process. This is because sodium hydroxide reacts with hemicellulose, and makes it easier to remove the hemicellulose under certain conditions. Sodium silicate emulsifies the fat and wax materials. Sodium sulfite decomposes lignin. Sodium pyrophosphate and sodium polyphosphate soften the fat, wax, and pectin. Compared with CPs-A, great changes were observed in the composition of CPs-B. The hemicellulose and lignin content decreased to 18.39% and 9.31%, respectively, while cellulose content increased to 65.44%. The results show that DMSO treatment can further remove non-cellulose substance in CPs, which is beneficial for the extraction of nanofibrillated cellulose (NFC). In order to explore the mechanism of DMSO for the preparation of nanofibers, the ethanol and acetone were used to deal with CPs according to the DMSO treatment conditions. The CPs with ethanol treatment is named CPs-C, while with acetone treatment is denoted as CPs-D. Compared with CPs-A, the chemical composition of CPs-C and CPs-D had some changes, but it was not as obvious as CPs-B. This indicates that ethanol cannot remove the non-cellulose substances in CPs, while acetone has a limited effect on the purification compared to DMSO. DMSO has the best effect on the further removal of non-cellulose substances among the three solvents.

Table 2. Chemical Composition of CHs and CPs

Sample	Wax (%)	Hydrotrope (%)	Pectin (%)	Hemicellulose (%)	Lignin (%)	Cellulose (%)
CHs	1.43±0.37	9.96±0.67	3.09±0.39	46.46±1.30	19.06±1.71	20.00±0.89
CPs-A	1.09±0.11	7.53±0.28	1.15±0.18	24.25±0.82	16.24±1.16	49.74±0.51
CPs-B	0.92±0.04	5.13±0.36	0.81±0.07	18.39±0.89	9.31±0.88	65.44±0.43
CPs-C	1.67±0.27	6.76±0.41	1.08±0.22	23.54±0.64	15.84±1.01	51.11±0.51
CPs-D	1.61±0.18	5.94±0.25	0.93±0.30	20.36±0.48	13.69±0.74	57.47±0.42

FTIR Analysis

The FTIR spectra were used to characterize the chemical groups of CHs, CPs-A, CPs-B, NFC-A, and NFC-B, as shown in Fig. 2. The broad absorption peaks centered between 3200 cm^{-1} and 3500 cm^{-1} are attributed to stretching of -OH groups; at around 2900 cm^{-1}, they are due to C-H stretching vibration. The peak at 1430 cm^{-1} is due to intermolecular hydrogen attraction at the C_6 group (Haafiz *et al.* 2014). The peak at 1370 cm^{-1} is related to the bending vibration of the C-H and C-O bonds in the polysaccharide aromatic ring, and the peak at 890 cm^{-1} is associated with β-glycosidic linkages between glucose units in cellulose (Mandal and Chakrabarty 2011). In addition, the broad absorption band at around 1040 cm^{-1} is due to the C-O-C pyranose ring stretching vibration. The absorption bands at the above wave-numbers are associated with the characteristics of native cellulose I (Haafiz *et al.* 2014). The spectra of CHs, CPs-A, CPs-B, NFC-A, and NFC-B had nearly the same absorption peaks in the above wave numbers, indicating that CPs-A, CPs-B, NFC-A, and NFC-B kept the structure of cellulose I after the chemical purification treatment, DMSO swelling, and the TEMPO oxidation process. The peak centered at 1730 cm^{-1} is attributed to the C=O stretching vibration of the acetyl and/or ketone groups of hemicellulose or carboxyl groups of lignin (Sun *et al.* 2005). The presence

of lignin is depicted by the band at 1500 cm^{-1}, which represents the aromatic C=C in plane symmetrical stretching vibration of the aromatic ring (Sun *et al.* 2005). The peak at around 1250 cm^{-1} represents the C-O out of plane stretching vibration of the aryl group in lignin (Haafiz *et al*. 2014). The absorption peak intensity decreased sharply or disappeared in the CPs-A, showing that hemicellulose and lignin were partly removed during chemical purification. Compared to the spectrum of CPs-A, the intensity of the absorption peaks in the CPs-B were further decreased in the above wave numbers, indicating that DMSO treatment can further remove the residual non-cellulose materials.

The absorption peak at 1162 cm^{-1} corresponds to C-C. The absorption peak at around 1107 cm^{-1} is attributed to the stretching vibration of C-O-C glycosidic ether bonds in cellulose (Mandal and Chakrabarty 2011). The C-O-C glycosidic ether absorption peak appears only in NFC-A and NFC-B spectra due to hydrolysis of polysaccharides during TEMPO oxidation. The absorption peaks at 1603 cm^{-1} were assigned to the O-C=O asymmetric stretching in CHs; the peak shifted to 1606 cm^{-1} and became sharper in the NFC-A and NFC-B spectra due to sodium carboxylate groups formed by TEMPO oxidation (Okita *et al.* 2011). The peak shape of NFC-B in the spectrum fits well with that of NFC-A, which indicates that there were no new functional groups in NFC-B after DMSO treatment.

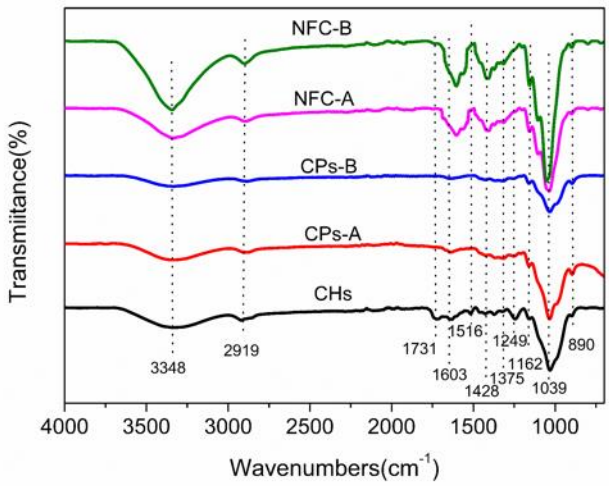

Fig. 2. FTIR spectra of CHs, CPs-A, CPs-B, NFC-A, and NFC-B

Zeta Potential Analysis

The dispersion stability of the NFC suspension was investigated by zeta potential analysis. The greater the absolute value of zeta potential, the better the dispersion stability of the NFC suspension. The zeta potential values of NFC-A and NFC-B were -51.5 mV and -67.8 mV, respectively. The hydroxyl groups on the surface of NFC were oxidized to carboxyl group during the TEMPO oxidation process, which gave the NFC a negative charge. The absolute value of zeta potential of NFC-B was bigger than that of NFC-A, reflecting that NFC-B had a bigger density of carboxyl groups. This was attributed to the ability of DMSO to partially dissolve and remove the residual non-cellulose substances that covered cellulose microfibrils, which made TEMPO reagents penetrate cellulose more easily and more hydroxyl groups were oxidized to carboxyl groups. The results reflect that DMSO treatment can improve the dispersion stability of NFC suspension.

Morphological Analysis

SEM was used to observe the morphology of cellulose samples, as shown in Fig. 3. The surface of CHs was uneven, and the fibers were wrapped by non-cellulose substances. Figure 3 (b) shows that CHs became fibrous, indicating most of the non-cellulose components were removed during the chemical purification. The image of CPs-A in Fig. 3 (c) demonstrates that cellulose fibers existed as aggregates of microfibers. The microfibers were further separated and degraded in CPs-B as the residual non-cellulose materials were further removed during DMSO treatment as shown in Fig. 3 (d).

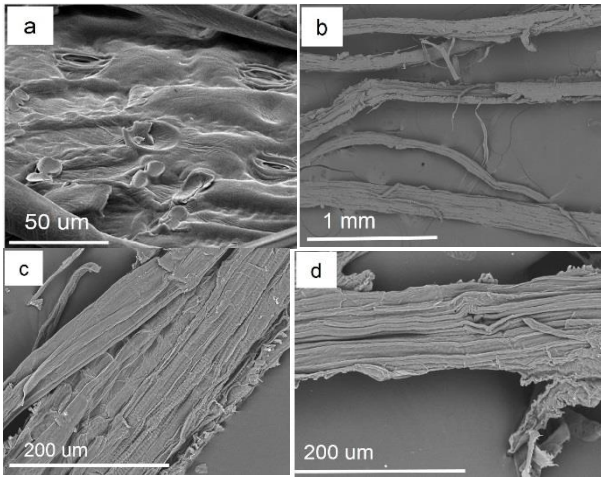

Fig. 3. SEM images of corn husks (a), cellulose fibers (b), CPs-A (c), and CPs-B (d)

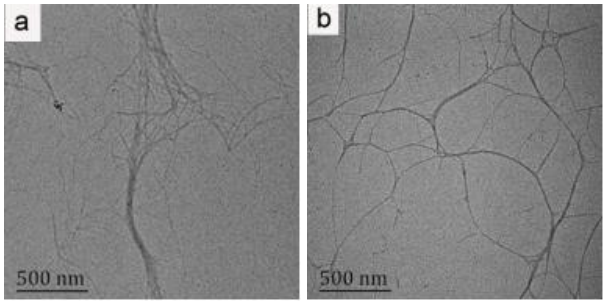

Fig. 4. TEM image of NFC-A (a) and NFC-B (b) isolated from corn husks

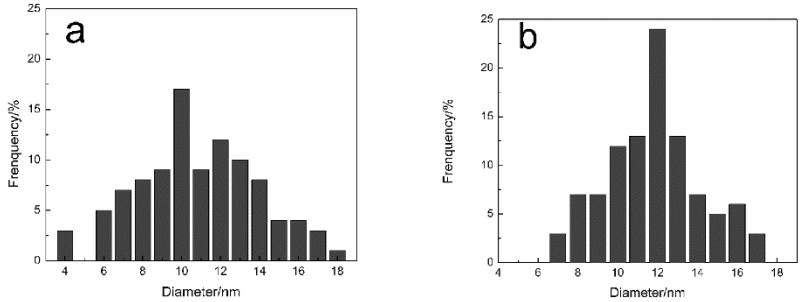

Fig. 5. Diameter-frequency histograms of (a) NFC-A and (b) NFC-B

TEM is the basic technique used to observe the morphology and distribution of NFC. Figure 4 shows the TEM image of NFC-A and NFC-B. Both NFC-A and NFC-B

were slender, on nanoscale, and distributed randomly. NFC-A exhibited an average diameter of 11.44 nm and a length from several hundred nanometers to several micrometers. Some NFC-A were aggregated and difficult to separate, while NFC-B had a much higher degree of dispersion with an average diameter of 10.48 nm and a length of several hundred nanometers.

Figure 5 shows the diameter-frequency histogram. The histograms indicate that the diameter of NFC-B had a narrower distribution range than NFC-A. The diameters of NFC-B were mainly distributed from 7 nm to 17 nm, while those of NFC-A ranged from 4 nm to 18 nm. These results indicate that although DMSO treatment is not an essential step during NFC extraction from corn husks, it affects the dimension and distribution of NFC.

X-Ray Diffraction Analysis

The crystallinity of CHs, CPs-A, CPs-B, NFC-A, and NFC-B was analyzed by X-ray diffractometry. Figure 6 illustrates that the diffraction peaks at 2θ =16.402°, 22.399°, and 34.798° observed for CPs-A, CPs-B, and NFC-A, NFC-B corresponded to the (110), (002), and (004) planes of cellulose I structure (Miao *et al.* 2016). This observation also indicated that the crystalline structure of cellulose I of CPs and NFC were maintained after chemical purification, DMSO treatment, and TEMPO oxidation. This was attributed to the fact that chemical purification removed most of the non-cellulose substances from CHs. DMSO treatment further removed hemicellulose and lignin, swelled the cellulose and broke inter-link hydrogen bonding, while TEMPO oxidation selectively oxidized some hydroxyl groups of cellulose to carboxyl groups. Therefore, chemical purification, DMSO treatment, and TEMPO oxidation did not change the cellulose polymorphs.

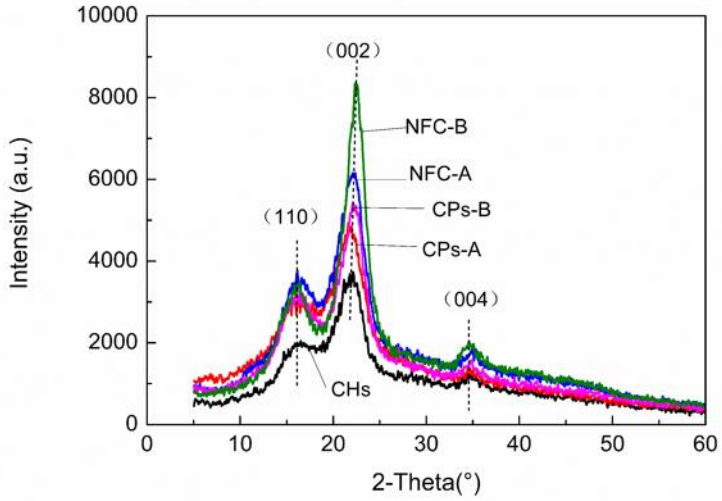

Fig. 6. X-ray diffraction spectrograms of CHs, CPs-A, CPs-B, NFC-A , and NFC-B

The crystallinity was calculated with the Segal method (Eq. 1) using the maximum intensity of the diffraction from the 002 plane (I_{002}), and the minimum intensity between the 002 and 110 peaks (I_{am}).

$$Cr(\%) = 100 \times (I_{002} - I_{am}) / I_{002} \quad (1)$$

Compared with CHs, the crystallinity of CPs-A was remarkably increased from 26.65% to 50.55%. This result was attributed to the removal of large amounts of hemicellulose, lignin, and other non-cellulose substances during chemical purification, which increased the cellulose content in CPs-A and improved the crystallinity. The crystallinity of CPs-B was further increased to 52.34%, showing that DMSO treatment can dissolve residual lignin and hemicellulose, leading to a further increase of the crystallinity of CPs-B. The diffraction peaks of NFC-A and NFC-B at 22.399° were sharper than in CPs-A and CPs-B, and the relative peak intensity increased. These results indicate the TEMPO oxidation increased the crystallinity of NFC, reflecting that TEMPO oxidation removes the amorphous and some defective crystallization regions of cellulose, which increased the crystallinity of NFC-A to 53.86%, and improved the crystallinity of NFC-B to 61.18%. The crystallinity of NFC-B is much bigger than that of NFC-A, showing non-cellulose materials that covered cellulose microfibrils could be further removed by DMSO treatment, which allowed the TEMPO reagents to penetrate cellulose samples more easily, and more amorphous area and defective crystallization regions could be removed by TEMPO oxidation.

Thermal Stability Analysis

The thermal stability of CHs, CPs-A, CPs-B, NFC-A, and NFC-B were investigated using thermogravimetric (TG) and derivative thermogravimetric (DTG) curves, as shown in Fig. 7. All samples presented an initial weight loss between 50 °C and 150 °C, mainly due to the loss of water and low molecular compounds. All samples had large weight degradation phenomenon in several stages. Thus, the samples contained a variety of substances with different degradation temperatures. The onset decomposition temperatures of CHs, CPs-A, CPs-B, NFC-A, and NFC-B occurred at 265 °C, 293 °C, 301 °C , 221 °C, and 247 °C, respectively. The maximum peak rates of degradation were reached at 369 °C, 377 °C, 379 °C, 251 °C, and 251°C, respectively, as revealed by DTG curves. Therefore, CPs-B had the highest thermal stability among the five samples.

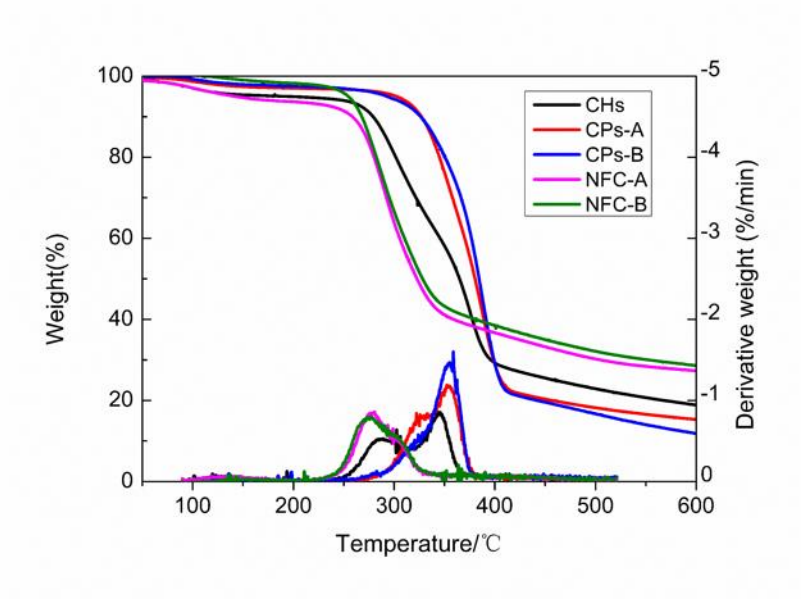

Fig. 7. TG and DTG curves of CHs, CPs-A, CPs-B, NFC-A, and NFC-B

CHs contained a higher content of molecules with lower thermal stability than cellulose, such as pectin, hemicellulose, and lignin, which caused the early degradation of CHs. However, the non-cellulose substances in CPs-A were mostly removed during chemical purification, which increased the onset degradation temperature. The residues non-cellulose material can be further dissolved or removed by DMSO treatment, leading to the increase of the onset degradation temperature of CPs-B. However, the onset degradation temperature of NFC was reduced. There are two reasons that may explain this phenomenon. First, during the process of TEMPO oxidation, the decrease in particle sizes and increase in specific surface area led to the increase in active groups on the surface, which reduced its thermal stability. Second, many cellulose chains were inevitably destroyed and fractured during TEMPO oxidation, which formed many low molecular weight chains and breaking points in the cellulose chains on the NFC surface and created many defects. The low molecular chains and defects on the surface of NFC absorbed heat and degraded gradually at lower temperatures, leading to the decreased thermal stability.

The DTG curve of CHs exhibits two degradation peaks. The first degradation peak occurred at 287 °C, representing non-cellulose component thermolysis, while the second degradation peak at 344 °C corresponded to cellulose degradation. Two degradation peaks also appeared in the DTG curve of CPs-A, but they were very close. Although most of non-cellulose substances were removed during chemical purification process, there were still a small amount of residues in CPs-A, leading to the existence of a small shoulder degradation peak before cellulose degradation. The residual non-cellulose composition were further removed during DMSO treatment. Therefore, only one degradation peak appeared in the DTG curve of CPs-B. There was only one degradation peak each in the DTG curves of NFC-A and NFC-B. The temperatures of onset degradation and the maximum degradation rate of NFC-B were higher than those of NFC-A, which indicates that the former had higher thermal stability. This is attributed to the fact that DMSO can remove the residue non-cellulose materials in CPs-A, which makes TEMPO reagents penetrate into CPs-B more easily. More amorphous area and defective crystallization regions in cellulose could be removed by TEMPO oxidation. As thermal stability of crystalline regions is much higher than that of amorphous area, the thermal stability of NFC-B was correspondingly improved.

CONCLUSIONS

1. Compared with ethanol and acetone, DMSO has a more obvious effect on the removal of non-cellulose materials, such as lignin and hemicellulose.
2. The mechanism of DMSO for the preparation of NFC by using TMEPO oxidation method is that DMSO treatment can partially dissolve or remove the non-cellulose substances that cover the cellulose microfibrils, which makes TEMPO reagents penetrate into cellulose more easily, leading to easier isolation of NFC.
3. The impact of DMSO on the morphology and properties of NFC was characterized by various techniques. DMSO treatment did not change the chemical function groups or cellulose polymorphs. However, DMSO treatment reduced the diameter of NFC from 11.44 nm to 10.48 nm with a narrower distribution range and changed the Zeta potential of NFC suspension from -51.5 mV to -67.8 mV. DMSO treatment also improved the crystallinity and thermal stability of NFC.

ACKNOWLEDGMENTS

The research reported in this paper was funded by Science and Technology Agency of Jiangsu Province (Project No. BE2014883) and Shanghai Municipal Education Commission (Project No. 14ZZ071). The work was also financially supported by the Fundamental Research Funds for the Central Universities (Project No.16D310102).

REFERENCES CITED

Barl, B., Biliaderis, C. G., Murray, E. D., and Macgregor, A. W. (1991). "Combined chemical and enzymic treatments of corn husk lignocellulosics," *J. Sci. Food. Agric.* 56(2), 195-214. DOI: 10.1002/jsfa.2740560209

Cao, X., Ding, B., Yun, J., and Al-Deyab, S. (2012). "Cellulose nanowhiskers extracted from TEMPO-oxidized jute fibers," *Carbohyd. Polym.* 90(2), 1075-1080. DOI: 10.1016/j.carbpol.2012.06.046

Carpenter, A. W., de Lannoy, C. F., and Wiesner, M. R. (2015). "Cellulose nanomaterials in water treatment technologies," *Environ. Sci. Technol.* 49(9), 5277-5287. DOI: 10.1021/es506351r

Chaker, A., Mutje, P., Vilar, M. R., and Boufi, S. (2014). "Agriculture crop residues as a source for the production of nanofibrillated cellulose with low energy demand," *Cellulose* 21(6), 4247-4259. DOI: 10.1007/s10570-014-0454-5

Do Nascimento, J. H. O., Luz, R. F., Galvao, F. M. F., Melo, J. D. D., Oliveira, F. R., Ladchumananandasivam, R., and Zille, A. (2015). "Extraction and characterization of cellulosic nanowhisker obtained from discarded cotton fibers," *Mater. Today-Proc.* 2(1), 1-7. DOI: 10.1016/j.matpr.2015.04.001

Du, C., Li, H., Li, B., Liu, M., and Zhan, H. (2016). "Characteristics and properties of cellulose nanofibers prepared by TEMPO oxidation of corn husk," *BioResources* 11(2), 5276-5284. DOI: 10.15376/biores.11.2.5276-5284

GB/T 5889 (1986). "Method of quantitative analysis of ramie chemical components," Standardization Administration of China, Beijing, China.

Grunert, M., and Winter, T. (2002). "Nanocomposites of cellulose acetate butyrate reinforced with cellulose nanocrystals," *J. Polym. Environ.* 10(1-2), 27-30. DOI: 10.1023/A:1021065905986

Haafiz, M. K. M., Hassan, A., Zakaria, Z., Inuwa, I. M., and Islam, M. S. (2014). "Isolation and characterization of cellulose nanowhiskers from oil palm biomass microcrystalline cellulose," *Carbohyd. Polym.* 103, 119-125. DOI: 10.1016/j.carbpol.2013.11.055

Isogai, A., Saito, T., and Fukuzumi, H. (2011). "TEMPO-oxidized cellulose nanofibers," *Nanoscale* 3(1), 71-85. DOI: 10.1039/c0nr00583e

Mandal, A. and Chakrabarty, D. (2011). "Isolation of nanocellulose from waste sugarcane bagasse (SCB) and its characterization," *Carbohyd. Polym.* 86(3), 1291-1299. DOI: 10.1016/j.carbpol.2011.06.030

Mendes, C. A. D., Ferreira, N. M. S., Furtado, C. R. G., and de Sousa, A. M. F. (2015). "Isolation and characterization of nanocrystalline cellulose from corn husk," *Mater. Lett.* 148, 26-29. DOI: 10.1016/j.matlet.2015.02.047

Miao, X. R., Lin, J. Y., Tian, F., Li, X. H., Bian, F. G., and Wang, J. (2016). "Cellulose nanofibrils extracted from the byproduct of cotton plant," *Carbohyd. Polym.* 136, 841-850. DOI: 10.1016/j.carbpol.2015.09.056

Moran, J. I., Alvarez, V. A., Cyras, V. P., and Vazquez, A. (2008). "Extraction of cellulose and preparation of nanocellulose from sisal fibers," *Cellulose* 15(1), 149-159. DOI: 10.1007/s10570-007-9145-9

Ng, H.-M., Sin, L. T., Tee, T.-T., Bee, S.-T., Hui, D., Low, C.-Y., and Rahmat, A. R. (2015). "Extraction of cellulose nanocrystals from plant sources for application as reinforcing agent in polymers," *Compos. Part B- Eng.* 75, 176-200. DOI: 10.1016/j.compositesb.2015.01.008

Okita, Y., Fujisawa, S., Saito, T., and Isogai, A. (2011). "TEMPO-oxidized cellulose nanofibrils dispersed in organic solvents," *Biomacromolecules* 12(2), 518-522. DOI: 10.1021/bm101255x

Saito, T., Kimura, S., Nishiyama, Y., and Isogai, A. (2007). "Cellulose nanofibers prepared by TEMPO-mediated oxidation of native cellulose," *Biomacromolecules* 8(8), 2485-2491. DOI: 10.1021/bm0703970

Salmela, M., Alén, R., and Vu, M. T. H. (2008). "Description of kraft cooking and oxygen-alkali delignification of bamboo by pulping and dissolving material analysis," *Ind. Crops. Prod.* 28(1), 47-55. DOI: 10.1016/j.indcrop.2008.01.003

Sun, X. F., Xu, F., Sun, R. C., Fowler, P., and Baird, M. S. (2005). "Characteristics of degraded cellulose obtained from steam-exploded wheat straw," *Carbohyd. Res.* 340(1), 97-106. DOI: 10.1016/j.carres.2004.10.022

Wang, H. K., Zhang, X. X., Jiang, Z. H., Li, W. J., and Yu, Y. (2015). "A comparison study on the preparation of nanocellulose fibrils from fibers and parenchymal cells in bamboo (*Phyllostachys pubescens*)," *Ind. Crops. Prod.* 71, 80-88. DOI: 10.1016/j.indcrop.2015.03.086

Xiao, S., Gao, R., Gao, L., and Li, J. (2016). "Poly(vinyl alcohol) films reinforced with nanofibrillated cellulose (NFC) isolated from corn husk by high intensity ultrasonication," *Carbohyd. Polym.* 136, 1027-1034. DOI: 10.1016/j.carbpol.2015.09.115

Yu, L., Lin, J., Tian, F., Li, X., Bian, F., and Wang, J. (2014). "Cellulose nanofibrils generated from jute fibers with tunable polymorphs and crystallinity," *J. Mater. Chem.* 2(18), 6042-6411. DOI: 10.1039/c4ta00004h

Zhang, D., Zhang, Q., Gao, X., and Piao, G. (2013). "A nanocellulose polypyrrole composite based on tunicate cellulose," *Int. J. Polym. Sci.* 2013(2013), 1-6. DOI: 10.1155/2013/175609

Article submitted: August 2, 2016; Peer review completed: October 15, 2016; Revised version received and accepted: November 3, 2016; Published: November 8, 2016.
DOI: 10.15376/biores.12.1.95-106